# Monte Carlo Simulation of Sorption Equilibria for Nitrogen and Oxygen on LiLSX Zeolite†

**Sudhakar R. Jale,* Martin Bülow, Frank R. Fitch, Naum Perelman, and Dongmin Shen**

*BOC Gases Technology, 100 Mountain Avenue, Murray Hill, New Jersey 07974*

*Received: October 25, 1999; In Final Form: March 29, 2000*

Grand canonical Monte Carlo simulation of sorption of nitrogen and oxygen has been carried out on LiLSX zeolite structures and accurate adsorption data was measured on LiLSX powder using the isosteric technique. The position of Li cations in the LiLSX structure was predicted using the MSI Cerius$^2$ cation locator module. Simulation of sorption on various structures of LiLSX, which contain Li cations at different locations, indicate that sites SIII and SIII′ show similar interaction energies and that Li cations in site SII are not involved in the sorption process. The simulated values for sorption capacity, $N_2/O_2$ selectivity and isosteric sorption heat are in good agreement with experimental data. The simulated values of sorption capacity and isosteric sorption heat on the predicted structures are also close to those obtained on structures built by using crystal structure data and the experimental sorption data obtained at low pressures.

## I. Introduction

The capability of molecular modeling to predict sorption performance of zeolites is being explored by many research groups due to its strong academic and industrial relevance.[1−4] Atomistic simulation allows for a calculation of sorption capacity and sorption heat at a given pressure, and it helps to explain the sorption phenomena on a microphysical level. Monte Carlo simulation provides a fast and effective tool for studying the sorption properties of zeolites. Simulation of the sorption behavior of various types of molecules in zeolites has been shown to yield results in excellent agreement with experimental data.[5,6] As far as low-molecular-weight gases are concerned, grand canonical simulations were carried out by Razmus and Hall[7] to predict the sorption isotherms of nitrogen ($N_2$), oxygen ($O_2$), and argon (Ar) on 5Å zeolite. A reasonably good agreement with experimental results was found. Later on, Watanabe et al.[8] have developed force field parameters by matching calculated Henry constants to those available from experimental data. This way, they achieved a better fit between simulated and experimental data for sorption processes of $N_2$ and $O_2$ on zeolite A. These potential parameters were embedded into the Molecular Simulation Inc. (MSI) Cerius$^2$ simulation package. This force field expression was extended to predict single and multicomponent sorption properties of $N_2$ and $O_2$ on zeolite LiX.[9] Sorption isotherms were predicted successfully over a wide range of pressures, viz., from 1 to 4 atm. Recently, Ligniéres and Pullumbi[10] have predicted the sorption isotherms of $N_2$ and $O_2$ on various zeolites, which agree, in general, with the experimental data but leave opportunities for further improvement. The data on heats of sorption was not published for the LiLSX system.

The separation of air by pressure/vacuum swing adsorption processes represents a large scale industrial application that utilizes lithium cation exchanged faujasite zeolites as sorbents.[11] Simulation of sorption equilibria for $N_2$ and $O_2$ on LiLSX zeolite is important in order to understand the thermodynamic limitations to process performance, and the influence of Li cation positioning on sorption capacity, $N_2/O_2$ selectivity, and sorption heat.[12] For a simulation of sorption properties, knowledge of the crystal structure of any zeolite under investigation is needed. Although a vast amount of work had already been done to determine the exact positions of cations in zeolites, it is almost impossible to determine the crystal structure of every zeolite with all possible cations, in particular, under the conditions of a real sorption process. However, development of computer modeling techniques is growing to successfully locate extra-framework cations in specific zeolite systems.[13,14] Although very good matches were found between simulation and crystal structure data for many structures, until now, no sorption simulations were carried out on those predicted structures.

The purpose of the current investigation is to study the sorption properties of $N_2$ and $O_2$ on LiLSX zeolite, and to compare theoretical sorption isotherms and isosteric sorption heats with experimental data. The influence of Li cation positioning at distinguished sites within the faujasite supercage on sorption performance of the zeolite is also investigated. Simulating sorption isotherms for those gases on a LiLSX structure, in which the positions of Li cations were predicted by means of the MSI cation locator module, is another purpose of this investigation.

## II. Simulation Methods

Since the energy of any system depends on the extent of deviation of bonds and angles from their equilibrium values, a force field expression consists, in general, of energy terms representing intra- and intermolecular forces. Because force field methods exclude electronic motions from the calculations, the energy expression for a molecule includes only the coordinates of individual atoms in a molecule. The force fields[15] which deal with zeolite frameworks constitute of all energy terms, such as bond stretching, angle bending, torsional terms, and non-bonded interactions. On the other hand, the force fields developed for sorption processes include only nonbonded interactions involving short range van der Waals and electrostatic (Coulombic) interactions.[8]

* Corresponding author: E-mail: sudhakar.jale@us.gtc.boc.com. Fax: (908) 771-6258. Internet: http://www.boc.com.

† The authors dedicate this paper to Professor Dr. Wolfgang Schirmer, Berlin-Hessenwinkel, Germany, on the occasion of his 80th birthday.

10.1021/jp993777r CCC: $19.00 
Published on Web 05/10/2000

**TABLE 1: Positions of Li Cations in Various LiLSX Structural Models Used for Sorption Simulations**

| structure | cell dimension, (Å) | SI′ | SII | SIII | SIII′ | ref |
|---|---|---|---|---|---|---|
| LiLSX-FL-III | 24.6957 | 32 | 32 | 32 | - | 18 |
| LiLSX-P-III+III′ | 24.6665 | 32 | 32 | 16 | 16 | 17 |
| LiLSX-P-III | 24.6665 | 32 | 32 | 32 | - | *a* |
| LiLSX-P-III′ | 24.6665 | 32 | 32 | - | 32 | *a* |

[a] Atomic coordinates reported in ref 17 were used to build the framework; 96 Li cations were added using MSI's cation locator module.

MSI's Cerius[2] 3.8 software was used to study physical sorption of $N_2$ and $O_2$ on LiLSX zeolite as a function of pressure. Calculations are based on the application of a Monte Carlo simulation algorithm in the grand canonical ensemble.[16] The procedure consists, in general, of placing sorbate molecules at random locations inside the zeolite cavity. Any random configuration of molecule positions is accepted with a probability that decreases exponentially with total interaction energy between the sorbate molecules and the host zeolite lattice (including cations). The zeolite framework is assumed to be rigid during the sorption process. Strictly speaking, the framework should be "relaxed" during sorption, but this would require extensive calculations, very much extended processing time, and a certain experimental information on specific sorption system behavior which is unavailable in the literature for almost all systems. The interaction potential parameters used in the force field expression of this investigation are published in the literature.[8]

It is worthwhile to mention that force field methods, which present the interaction energy as sum of two independent parts (van der Waals and Coulombic), cannot be rigorously justified from the fundamental quantum-mechanical approach for small distances between species typical for sorption processes under consideration. Therefore, it is natural to consider the values such as effective charges and quadrupole moments as adjustable parameters to fit the sorption experimental data rather than fundamental constants that can be taken from published experimental measurements unrelated to the sorption processes. Also it can be expected that with decrease in characteristic distances between species (at elevated pressures, for instance) the quantum-mechanical effects are of increased significance resulting in more limited accuracy of the "classical" force field approach.

## III. Zeolite Structures

The structures of LiLSX zeolite were built using literature data, as summarized in Table 1. According to Plevert et al.,[17] sites SI′ and SII are fully occupied, and the cations in a supercage are equally distributed between SIII and SIII′ sites. The site SIII is ascribed to the center of four-membered ring in the supercage, while the SIII′ site is located near to the edge of four-membered ring in the 12-ring pore opening window as shown in Figure 1. As summarized in Table 1, this structure was described as LiLSX-P-III+III′. To study the influence of the position of cations in SIII and SIII′ sites, two more structures were built by placing 32 cations in either SIII or SIII′ site. These structures were named as LiLSX-P-III and LiLSX-P-III′, respectively. Like the original structure proposed by Plevert et al., both of these structures contain 32 Li cations in each of SI′ and SII sites. Feuerstein and Lobo[18] have used neutron diffraction and Li MAS NMR to predict the structure of dehydrated LiLSX. In contrast to Plevert et al., they did not find any Li cations in the SIII′ site. The site SIII as proposed by Feuerstein and Lobo is at the corner of four-ring window rather than at the center, as proposed by Plevert et al. Although the position of only 23 Li cations was determined by neutron diffraction by Feuerstein and Lobo, 32 cations were ascribed to SIII site. This system was designated as LiLSX-FL-III as reported in Table 1.

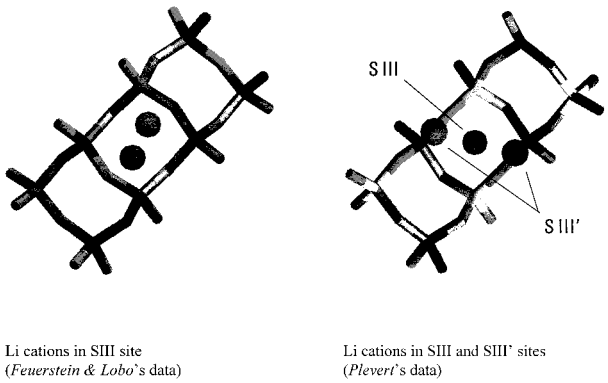


**Figure 1.** Comparison of the positioning of Li cations in different models.

Lithium cations in I′ and II sites are near the center of the six-membered window in all these structures. However, site SIII of the Plevert model is at the center of the four-membered ring, while, in the Feuerstein and Lobo model, it is at the corner of four-membered ring as depicted in Figure 1. The lithium cations in the above structures were distributed uniformly in such a way that no adjacent SIII and SIII′ cations are present. The sodalite cages were blocked by large "dummy" atoms to avoid creation of $N_2$ and $O_2$ sorbate molecules in these cages. One simulation comprised always one million iterations.

The quadrupole moments of $N_2$ and $O_2$ were set to $-1.2 \times 10^{-26}$ and $-0.40 \times 10^{-26}$ esu, respectively, using a three-site point charge model. The central "dummy" atoms in $N_2$ and $O_2$ were given a charge, $+0.810$ and $+0.224$, respectively. The charge on framework oxygen was set to $-1.00$. However, the charge on Li cations was varied to match the simulated data with experimental results, while the charges on silicon and aluminum ions were adjusted to maintain the charge neutrality. Since all of aluminum and silicon atoms are buried by framework oxygen atoms and do not contribute to the sorption process, as described earlier,[8,9] the identical charge was ascribed to these two types of atoms.

## IV. Experimental Section

Experimental sorption thermodynamic data of $N_2$ and $O_2$ on LiLSX zeolite were derived from directly measured sorption isosteres for the two systems. For this purpose, a modern isosteric method had been used. This method was described previously in detail.[12] Its principle is to measure the equilibrium pressure as a function of temperature, while a constant sorption phase concentration is maintained in a system with minium dead volume. Sorption thermodynamic functions are obtained from the linear relationship between equilibrium pressure ($\ln p$) and temperature ($1/T$) for a given sorption phase concentration. By repeating the procedure for various concentrations, a full set of sorption thermodynamic quantities, such as the isosteric sorption heat and the sorption entropy as functions of sorption phase concentration can be determined. Of those data, the low concentration range of the isosteric sorption heats will be discussed in this paper.

The LiLSX zeolite of this investigation was synthesized in our laboratory. The powder was pelletized without any binder and sieved into a size faction of *c.* (1.5−2.0) mm diameter.

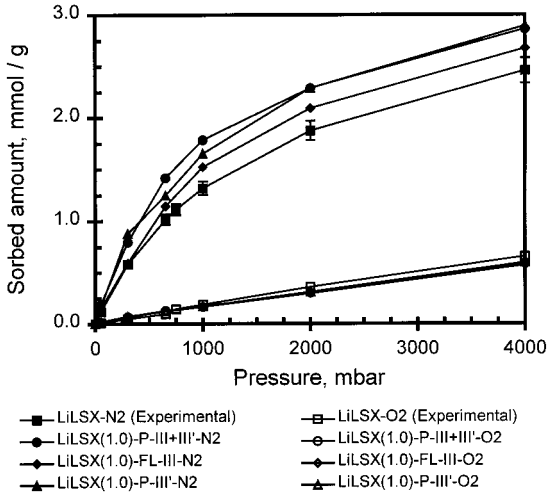


**Figure 2.** Comparison of experimental and simulated sorption isotherms of nitrogen and oxygen on LiLSX. The charges were $q_{Li} = 1.0$, $q_{Al}$ and $q_{Si} = 1.50$, and $q_O = -1.0$. Both experimental and simulated data sets were obtained at 298 K.

The LiLSX pellets weighing about 5.7 g (dry weight) were used for the isosteric measurements. The sample was activated in situ by slowly elevating the temperature to 400 °C during a period of 48 h in vacuo and keeping it at 400 °C for ca. 12 h. Experimental isosteric $N_2$ sorption heats presented in this paper were measured under the following experimental conditions: sorption phase concentrations from 0.0225 to 10.3789 mol/kg (exceeding saturation capacity), equilibrium pressures from 0.097 to 96.201 Torr, and temperatures from 67 to 292 K. For $O_2$, these conditions were as follows: sorption phase concentrations from 0.2268 to 12.7458 mol/kg (exceeding saturation capacity), equilibrium pressures from 0.111 to 96.473 Torr, and temperatures from 50 to 164 K.

## V. Results and Discussion

Simulation of sorption behavior was performed at 298 K on LiLSX-P-III+III′, LiLSX-P-III′, LiLSX-P-III, and LiLSX-FL-III structures, which contain Li cations at different locations. The simulated sorption isotherms of $N_2$ and $O_2$ for various LiLSX structures that contain Li cations with + 1.0 charge are plotted in Figure 2. For comparison, the experimental sorption data as obtained in our laboratory and data as reported in the literature,[11,19,20] have been summarized and shown with error bars. Although, the Li/Al ratio of the LiLSX samples reported in the literature is equal to 1.0, a deviation of about 5% in $N_2$ capacities was observed. However, these differences are not significant if considering possible differences in quality between real LiLSX samples. Values of sorption uptake of $N_2$ are always higher than those of $O_2$, due to the higher quadrupole moment of the former sorbing species. Values of simulated $N_2$ sorption capacity are found to be higher than the corresponding experimental data, for all structures. The LiLSX structures, built using the data of Plevert et al., yield slightly higher values of sorption capacity as compared to those for structures built by means of the Feuerstein and Lobo model. The simulated values for loading of all the four structures with $O_2$, are in very good agreement with experimental data, particularly, for low values of equilibrium pressure. Since the interaction between $O_2$ and cations is very weak due to the comparatively small value of the $O_2$ quadrupole moment and its weak interaction with the electric field gradient created by the cations, there is a negligible influence of the position of Li cations on sorption uptake of $O_2$.

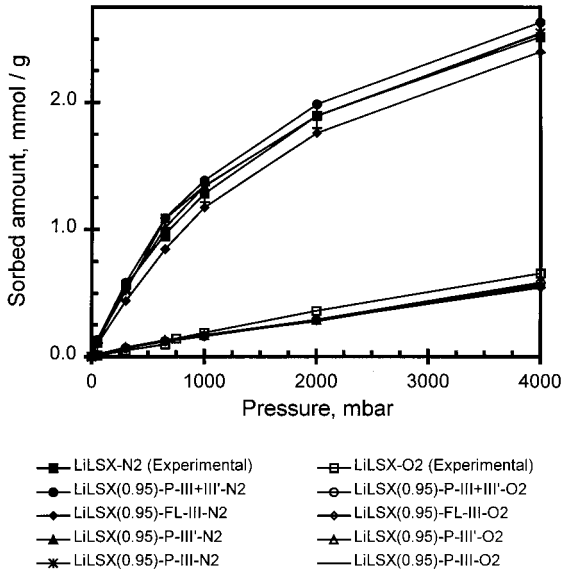


**Figure 3.** Comparison of experimental and simulated sorption isotherms of nitrogen and oxygen on LiLSX. The charges were $q_{Li} = 0.95$, $q_{Al}$ and $q_{Si} = 1.525$, and $q_O = -1.0$. Both experimental and simulated data sets were obtained at 298 K.

**TABLE 2: Positions of Li Cations in Various LiLSX Structural Models as Generated by Means of the Cation Locator**

| | atomic charges | | | | | | |
|---|---|---|---|---|---|---|---|
| structure | Si | Al | O | SI′ | SII | SIII | SIII′ |
| LiLSX-FL-Si1.5Al1.5 | 1.50 | 1.50 | −1.0 | 32 | 32 | 32 | - |
| LiLSX-FL-Si2.05Al1.75 | 2.05 | 1.75 | −1.2 | 32 | 32 | 16 | 16 |
| LiLSX-FL-Si2.4Al1.4 | 2.40 | 1.40 | −1.2 | 32 | 32 | 2 | 30 |
| LiLSX-P-Si1.5Al1.5 | 1.50 | 1.50 | −1.0 | 32 | 32 | 32 | - |
| LiLSX-P-Si2.05Al1.75 | 2.05 | 1.75 | −1.2 | 32 | 32 | 22 | 10 |
| LiLSX-P-Si2.4Al1.4 | 2.40 | 1.40 | −1.2 | 32 | 32 | 2 | 30 |

As demonstrated earlier for Ca and Na cations,[8] a way to match the simulated data with experimental results might be to reduce the charge on Li cation. Notwithstanding the fact that Li cation needs to have a charge, + 1.0, to compensate the framework's negative charge, experimentally, the effective charge on Li cation might be reduced due to a certain shielding of cations by partial hydration and by framework oxygen atoms, as well as due to an influence of charge transfer from framework oxygen atoms toward the cations. Taking into account such a situation, the charge on Li cations within all models was changed to a value of + 0.95, while charge neutrality was achieved by adjusting the charges of silicon and aluminum, correspondingly.

The simulated sorption uptakes of all three structures having Li with +0.95 charge are plotted in Figure 3. It can be clearly seen that the $N_2$ sorption uptakes on LiLSX-III+III′, LiLSX-P-III, and LiLSX-P-III′ structures are in very good agreement with the experimental data, particularly at lower pressures. The LiLSX-FL-III structure exhibits slightly lower loadings. However, when the charge on Li cations was increased from +0.95 to +0.97, the simulated $N_2$ sorption isotherm on LiLSX-FL-III also matches very well with the experimental data. These minor differences among these three structures could be due to the influence of screening by framework oxygens on Li cations at different locations.

The simulated values of $O_2$ loading on all four structures are in good agreement with experimental data in a low pressure region, but they deviate slightly from each other at high pressures. The values of sorption capacity for $N_2$ and $O_2$, and of the $N_2/O_2$ selectivity were calculated for all the structures at

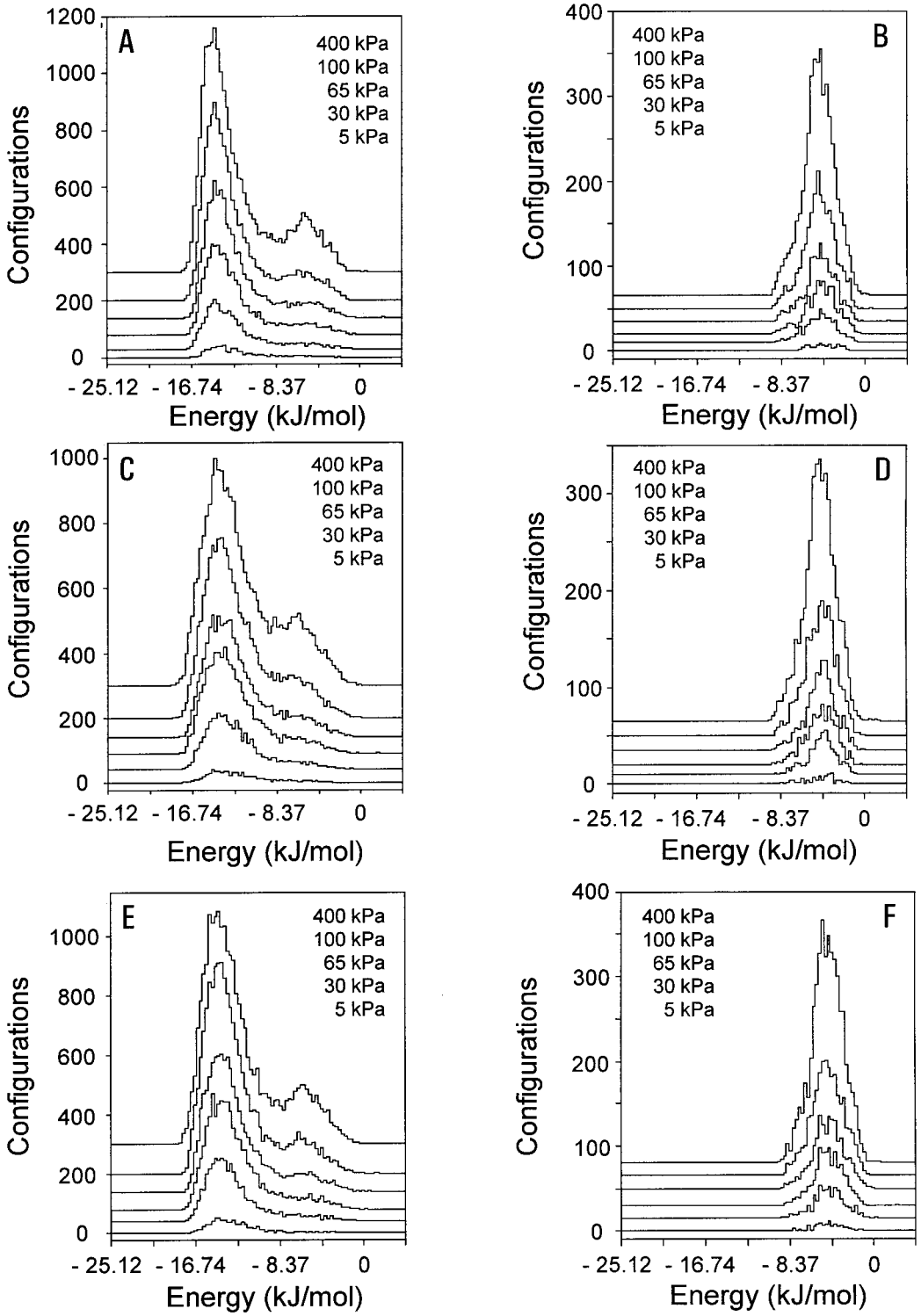


**Figure 4.** Distribution of potential energies for sorption of nitrogen and oxygen on various LiLSX structures. Simulations were performed at 298 K and 100 kPa. The charges were: $q_{Li} = 0.95$, $q_{Al}$ and $q_{Si} = 1.525$, and $q_O = -1.0$. (A) LiLSX-FL-III/$N_2$, (B) LiLSX-FL-III/$O_2$, (C) LiLSX-P-III+III′/$N_2$, (D) LiLSX-P-III+III/$O_2$, (E) LiLSX-P-III′/$N_2$, (F) LiLSX-P-III′/$O_2$.

1000 mbar pressure. They are compared with the experimental data in Table 2. Obviously, the simulated values for the $N_2$ capacity are very similar to the experimental results. However, simulations underestimate the zeolite capacity for $O_2$ which leads to slightly higher theoretical values for the $N_2/O_2$ selectivity. Taking into account the differences between experimental data obtained in various laboratories, the simulation results should be considered as being in excellent agreement with experimental results.

The distribution of potential energies for sorption of $N_2$ and $O_2$, at different values of sorption equilibrium pressure, are plotted in Figure 4. Since stronger sorption of a species results in a more negative value of energy, as shown in the plots, more negative energy values correspond to stronger sorption interaction energy. Obviously, sorption of $N_2$ is much stronger (lower value of potential energy calculated) than that of $O_2$, and this results in two energetically distinct sorption sites. This is also evident from the distribution of sorption sites as plotted in Figures 5A,B for $N_2$ and $O_2$, respectively. Nitrogen sorption is localized at the low-energy site (due to Coulombic interaction),

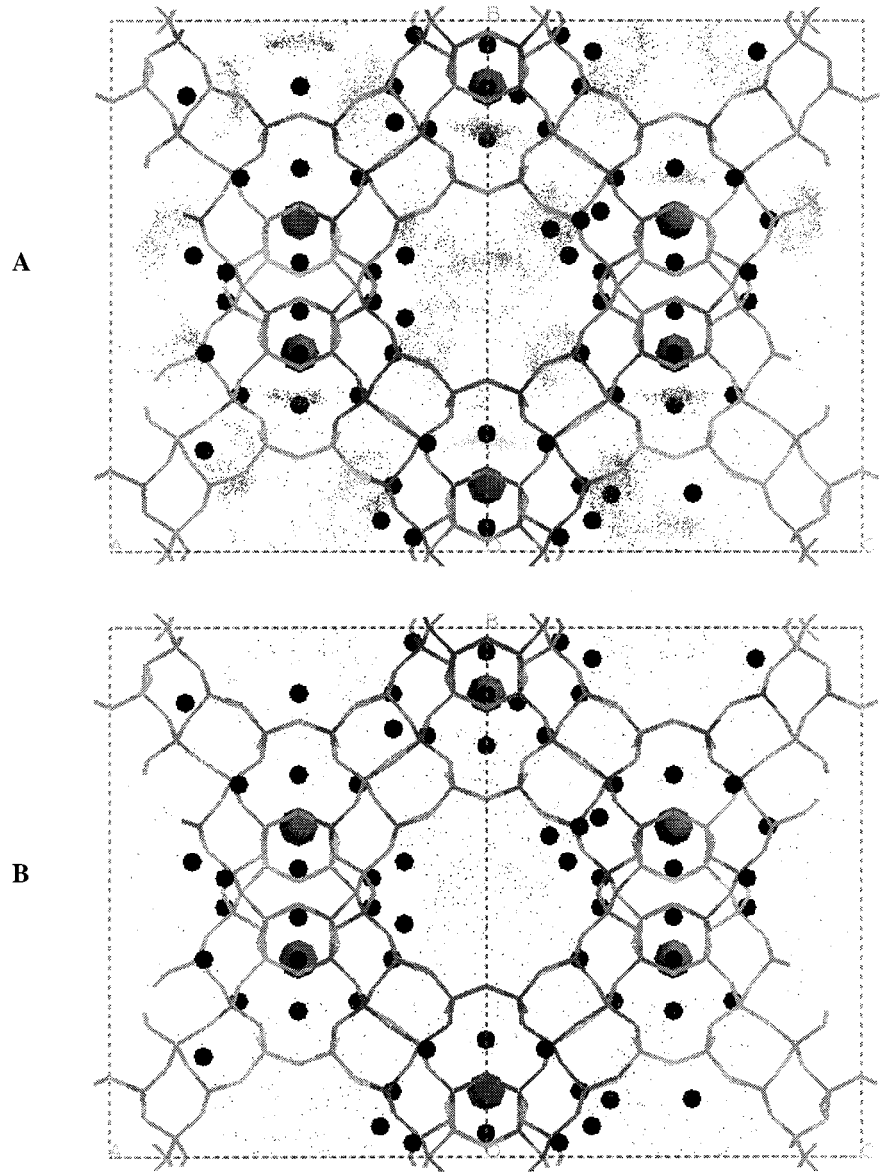


**Figure 5.** (A) Simulation results for the distribution of nitrogen sorption sites in LiLSX. Simulations were performed at 298 K and 100 kPa. The charges were $q_{Li} = 0.95$, $q_{Al}$ and $q_{Si} = 1.525$, and $q_O = -1.0$. (B) Simulation results for the distribution of oxygen sorption sites in LiLSX. Simulations were performed at 298 K and 100 kPa. The charges were $q_{Li} = 0.95$, $q_{Al}$ and $q_{Si} = 1.525$, and $q_O = -1.0$.

which is close to the cations in site SIII or SIII′. The high-energy sites (due to van der Waals interaction) are distributed homogeneously near the oxygen atoms of zeolite framework. Because of its small quadrupole moment, the $O_2$ sorption is dominated by the Lennard-Jones term. This leads to a fairly uniform distribution without any specific sorption sites. Similar results have been published for sorption of $N_2$ and $O_2$ on CaA zeolite.[21] The higher contribution of van der Waals vs Coulombic interaction in the case of $O_2$ is further confirmed either by switching off the Coulombic term in the Cerius software or by defining zero charges for all atoms in a three-site point charge model. Without Coulombic term, at 1000 mbar pressure, the nitrogen loading goes down by about 90% and that of oxygen by about 35%. This clearly indicates that nitrogen sorption is dominated by Coulombic interactions while oxygen sorption is dominated by van der Waals interactions.

Because of some shielding by framework oxygen atoms, Li cations in SII site were ruled out as possible sorption centers.[22] The analysis of mass distribution plots (Figure 5) suggests that the Li cations in site SII do not interact preferably or strongly with $N_2$ species. Since there is only one energy site for Coulombic interactions, cf., Figure 4, in all LiLSX structures, the sites with lowest potential energy, i.e., highest sorption interaction energy, can be attributed to Li cations in SIII and SIII′ sites. Similar values of sorption energy obtained for various LiLSX models that contain Li cations at different locations in their supercages, indicate that the sites SIII and SIII′ are energetically equivalent. The data for isosteric sorption enthalpy presented in a later section supports this conclusion. The plot of $N_2$ sorption energies suggests that sorption takes place preferentially at the lowest energy sites (stronger sites) and is negligible at higher energy sites (weaker sites) at low pressures. Nitrogen or oxygen sorption uptake at nonselective sites that belong to framework oxygen atoms, increases with pressure. This explains why values of $N_2/O_2$ selectivity were higher at low pressure and decrease with increasing pressure.

**Cation Locator.** Molecular Simulations Inc.[23] has developed a method to determine positions of nonframework cations based on Monte Carlo packing and structure optimization techniques. This module, designated as "cation locator" in the Cerius[2] package, uses an efficient grid-based algorithm to identify potential energy minima to place cations inside the zeolite

framework. A three-dimensional periodic reference grid with a spacing of (0.25−0.5) Å will be first constructed on the framework under investigation. A secondary cation reference grid will also be constructed with identical dimensions to the framework reference grid. The interaction of a selected cation with the framework will be calculated at each grid point using nonbonded interactions that include short-range van der Waals interactions with a cutoff of 5.5 Å, and long-range electrostatic interactions calculated using an Ewald summation. Symmetry rules are applied to speed up the calculation. The cations will be added one by one to the lowest energy grid sites. Once a required number of cations is added, a full or partial geometry optimization will be done using appropriate interatomic potentials.

Lithium cations were removed from the LiLSX structures as per the Feuerstein and Lobo (LiLSX-FL-III) and Plevert et al. (LiLSX-P-III+III′) models, and 96 Li cations were added to each of these structures using the cation locator at a grid spacing of 0.25 Å. The charge on Li cation was fixed at a value, + 1.0, while the charges on framework atoms (oxygen, silicon, and aluminum) were adjusted to maintain charge neutrality. Newsam et al.[13] and Mellot and Cheetham[14] have used a charge difference of 1.0, while Jaramillo and Auerbach[24] have used a difference of only 0.3 with a charge of − 1.2 on framework oxygen. In the current investigation, simulations were carried out using a charge difference of 0.3 and 1.0 between Si and Al in LSX structures built by using the crystal structure data published by Plevert et al. and Feuerstein and Lobo. Simulations were also performed on structures, which contain the same charge on both Si and Al ($q_{Si}$ and $q_{Al}$ = +1.5) with a − 1.0 charge on framework oxygen. Since the interaction between cations and zeolite framework is very strong, it is appropriate to distinguish between charges for Si and Al, although this will have less influence on sorption simulation.

The simulation results are summarized in Table 2. The structures generated using the framework data by Plevert et al., was designated as LiLSX-P. Those generated by means of the Feuerstein and Lobo model were designated as LiLSX-FL. The charges attributed to the Si and Al atoms were added to the end of the corresponding label. For example, in LiLSX-P-Si2.4Al1.4, the framework is built by Plevert et al. data, with charges on Si and Al atoms that amount to 2.4 and 1.4, respectively. If the charge difference between Si and Al amounts to 1.0, Li cations prefer SIII′ sites, while they prefer SIII site if their charge is the identical. At a charge difference of 0.3, Li cations were placed at both SIII and SIII′ sites. If the charge on both Si and Al is identical, the Li cation was placed at the center of four-membered ring, where it experiences identical interaction from all directions and, hence, the preferred site would be SIII. However, if the charge difference between Si and Al is increased, the Li cation moves to the corner of the four-membered ring, i.e., to the SIII′ site, near the aluminum. These results indicate that the population of Li cations at site SIII′ can be increased by increasing the charge difference between Si and Al of the LSX structure. Choosing the optimal charge set depends on what should be the final structure. If the LiLSX structure reported by Plevert et al. has to be obtained, the charges on Si and Al should be set to 2.05 and 1.75, respectively. On the other hand, if one wants to build the structure reported by Feuerstein and Lobo, the charge on both Si and Al should be 1.5. It is also important to mention that the charge difference between Si and Al does not have much influence on the position of Li cation at sites SII and SI′.

Recently, Mellot and Cheetham predicted the position of Li cations in LiLSX by energy minimization methods.[14] The

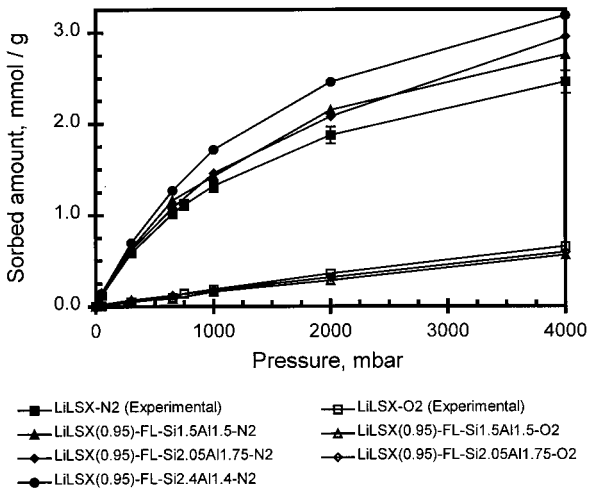


**Figure 6.** Comparison of simulated nitrogen and oxygen sorption isotherms of LiLSX-FL structures built by means of the cation locator module, with the experimental data of LiLSX. The charges were $q_{Li}$ = 0.95, $q_{Al}$ and $q_{Si}$ = 1.525, and $q_O$ = −1.0. Both experimental and simulated data sets were obtained at 298 K.

starting structure was built using the crystal structure data published by Plevert et al. and by attributing additional 32 Li cations to each type of SI′ and SII sites. The remaining 32 missing Li cations were randomly added into the supercage. The sodalite cages were blocked by large "dummy" atoms to avoid an insertion of Li cations into them. At a fixed framework structure, all 32 Li cations were placed in SIII′ sites. In this manuscript, the partial charges on the zeolite structure were (Si) +2.4 (Al) +1.4; (O) −1.2; and (Li) +1.0. As reported earlier, the simulations performed in this study using the cation locator led to similar results (Table 2), when identical charges were used.

Beside attributing a cation to a given site, it is equally important to know the exact position of the cation at that site, in order to assess quantitatively the sorption properties of the given system. For example, a Li cation at site SIII could be at different distances from the plane of the four-membered ring. Similarly, as shown in the literature,[25] there will be many positions for a cation at site SIII′. These differences may have significant consequences for particular sorption phenomena.

After locating the position of cations, "blocking" atoms were added into sodalite cages. This is to avoid creation of sorbing species in inaccessible sites. Since the interaction between the framework and cations in a zeolite is much stronger than that between the zeolite framework and sorbing species, the influence of a charge difference between Si and Al will have a significant effect on simulating the position of cations but it does not have much effect on sorption simulations. Hence, although different charges were used to locate the cation positions, based on the published force field model, the following charges were ascribed to Li cations and framework elements for sorption simulations: $q_{Si}$ and $q_{Al}$ = +1.525, $q_O$ = −1.0, and $q_{Li}$ = 0.95.

Monte Carlo sorption simulations were performed on all the previously described structures at a temperature of 298.15 K. The results are plotted in Figures 6 and 7. Values of sorption capacity and $N_2/O_2$ selectivity as calculated at a pressure of 1000 mbar are summarized in Tables 3 and 4. The structures that contain Li cations in sites SIII′ show higher sorption capacities than those that contain Li cations in sites SIII or in both sites SIII and SIII′. With some minor discrepancies, these results are similar to those obtained on LiLSX structures built by using crystal structure data. Therefore, the Feuerstein and Lobo

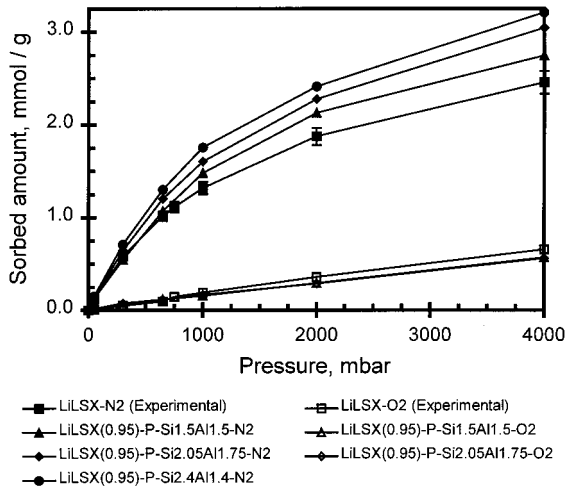


**Figure 7.** Comparison of simulated nitrogen and oxygen sorption isotherms of LiLSX-P structure, built by means of the cation locator module, with the experimental data for LiLSX. The charges were $q_{Li} = 0.95$, $q_{Al}$ and $q_{Si} = 1.525$, and $q_O = -1.0$. Both experimental and simulated data sets were obtained at 298 K.

**TABLE 3: Comparison of Simulated and Experimental Values of Sorption Capacity for Nitrogen and Oxygen**

| structure | loading at 1000 mbar (mmol/g) $N_2$ | loading at 1000 mbar (mmol/g) $O_2$ | $N_2/O_2$ selectivity |
|---|---|---|---|
| LiLSX (experiment) | 1.320 | 0.188 | 7.0 |
| LiLSX-FL-III | 1.171 | 0.161 | 8.5 |
| LiLSX-P-III+III′ | 1.386 | 0.164 | 8.0 |
| LiLSX-P-III | 1.341 | 0.168 | 8.0 |
| LiLSX-P-III′ | 1.339 | 0.169 | 7.9 |

**TABLE 4: Values for Sorption Capacity and $N_2/O_2$ Selectivity of LiLSX Structures for Which the Positions of Li Cations Were Determined by Means of the Cation Locator**

| structure | loading at 1000 mbar (mmol/g) $N_2$ | loading at 1000 mbar (mmol/g) $O_2$ | $N_2/O_2$ selectivity |
|---|---|---|---|
| LiLSX (Experiment) | 1.320 | 0.188 | 7.0 |
| LiLSX-FL-Si1.5Al1.5 | 1.423 | 0.161 | 8.8 |
| LiLSX-FL-Si2.05Al1.75 | 1.459 | 0.180 | 8.1 |
| LiLSX-FL-Si2.4Al1.4 | 1.716 | | |
| LiLSX-P−Si1.5Al1.5 | 1.481 | 0.159 | 9.3 |
| LiLSX-P−Si2.05Al1.75 | 1.606 | 0.164 | 9.8 |

structure that contains Li cations at site SIII showed a lower capacity than the Plevert et al. structure which contains Li cations in both SIII and SIII′ sites. All structures generated by the cation locator exhibited higher values of $N_2$ sorption capacity than those structures that were built on the basis of "genuine" crystal structure data. These discrepancies can be ascribed mainly to minor differences in positioning the Li cations at either SIII or SIII′ sites. Since the interaction of $O_2$ with the zeolite framework is predominantly governed by van der Waals interactions, the values of $O_2$ sorption uptake are not influenced that strongly by differences in the cation positions. The simulated values of sorption uptake for $N_2$ are close to the experimental data at lower pressure values, but they deviate significantly from the latter at higher pressures. A small difference in unit cell dimensions between the LiLSX-FL and LiLSX-P structures, which leads to slight changes in bond lengths and angles, may also contribute to the occurrence of minor differences in values of sorption capacity of these structures.

**Isosteric Sorption Heat.** Another result of the Monte Carlo simulation of sorption processes comprises differential sorption heats. This fundamental parameter is calculated from the slope of curves obtained by plotting the total potential energy vs the amount sorbed. The isosteric sorption heat, $\Delta H_{st}$, can then be calculated by adding the mechanical function to the differential sorption heat, $\Delta H_D$, assuming that the gas is ideal and the sorption phase is denser than the gas.[1] Simulated isosteric sorption heats for $N_2$ and $O_2$ on various LiLSX structures that contain Li cations with the charge, + 0.95, are plotted against the sorption phase concentration in Figure 8. For comparison, the experimental data are also plotted in Figure 8. As expected, $\Delta H_{st}$ decreases gradually with increasing sorption phase concentration, for both simulated and experimental data. However, the simulated values of $\Delta H_{st}$ are somewhat higher than the experimental data. This difference increases with sorption phase concentration and amounts to about 2 kJ/mol, at the most. Furthermore, the sorption heats for LiLSX structures, LiLSX-P-III + III′ and LiLSX-P-III, that contain Li cations in the center of four-membered rings, i.e., in site SIII, are higher than those for the structures, LiLSX-P-III′ and LiLSX-FL-III, that contain Li cations either at the corner of four-membered rings (site SIII of the Feuerstein and Lobo model), or close to 12-membered ring windows, i.e., site SIII′. In fact, the values of $N_2$ sorption capacity of a LiLSX structure that contain Li cations in site SIII were lower than those for structures that have cations in either SIII′ or in both SIII and SIII′ sites. However, these differences do not seem to be very significant.

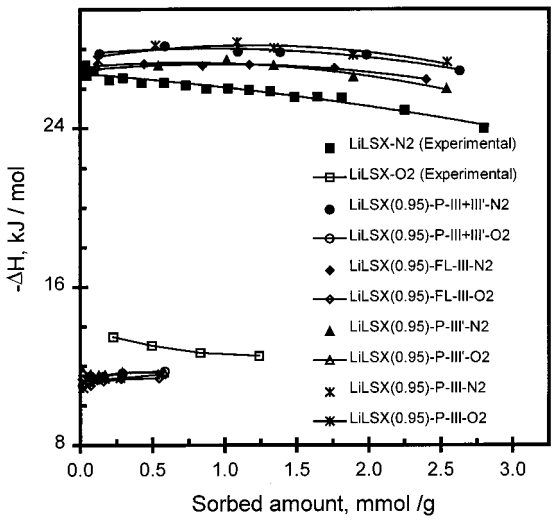


**Figure 8.** Comparison of experimental and simulated isosteric sorption heats for nitrogen and oxygen on LiLSX. The following charges were used: $q_{Li} = 0.95$, $q_{Al}$ and $q_{Si} = 1.525$, and $q_O = -1.0$.

Simulated values of the isosteric sorption heat for $O_2$ is found to be almost the same on all those structures. Since the contribution of Coulombic interactions between $O_2$ molecules and cations is relatively weak, the sorption heat of $O_2$ is much lower than that of $N_2$. For the same reason, there is a negligible influence of the position of Li cation on the isosteric sorption heat for $O_2$. Values of the simulated and experimental sorption heats of $O_2$ are compared to each other in Figure 8. It is also noteworthy that simulations tend to underestimate the strength of interactions between the zeolite and $O_2$ molecules.

The isosteric sorption heats of $N_2$ and $O_2$ for LiLSX structures built by means of the cation locator module, viz., LiLSX-P and LiLSX-FL, are plotted as concentration dependencies in Figures 9 and 10. Despite some differences in values of sorption capacity of those structures for $N_2$, the isosteric sorption heats of both structures are very close to each other. Again, in analogy to the structures built using crystal structure data, viz., LiLSX-FL-III and LiLSX-P-III+III′, the simulated sorption heat of $N_2$ is slightly higher for all the simulated LiLSX structures as

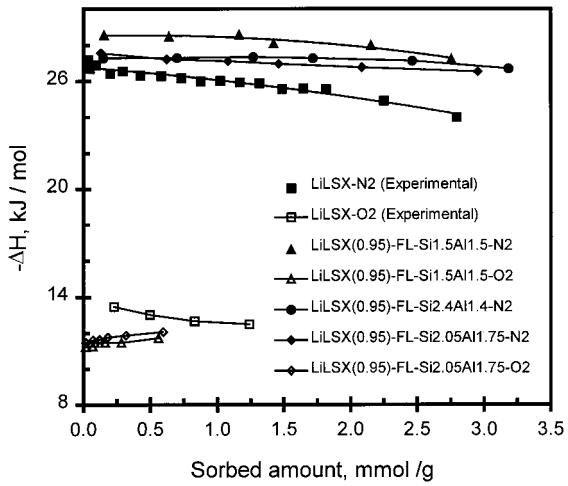


**Figure 9.** Comparison of simulated isosteric sorption heats for nitrogen and oxygen on the LiLSX-FL structure built by means of the cation locator module, with experimental data. The following charges were used: $q_{Li} = 0.95$, $q_{Al}$ and $q_{Si} = 1.525$, and $q_O = -1.0$.

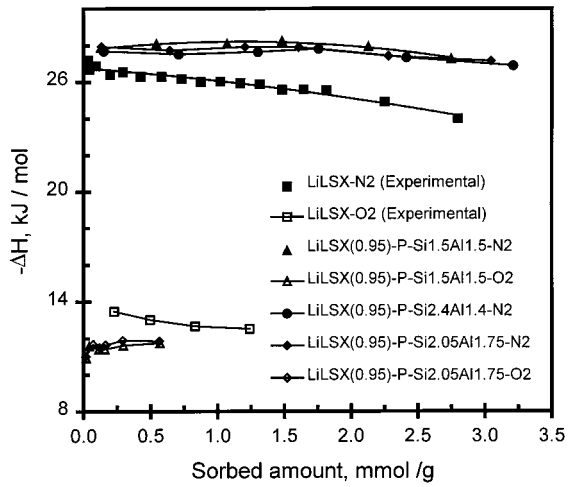


**Figure 10.** Comparison of simulated isosteric sorption heats for nitrogen and oxygen on the LiLSX-P structure as built by means of the cation locator module, with the experimental data. The following charges were used: $q_{Li} = 0.95$, $q_{Al}$ and $q_{Si} = 1.525$, and $q_O = -1.0$.

compared with the experimental isosteric sorption heat and is lower for the $O_2$ systems.

**Studies on Binary Mixtures of Nitrogen and Oxygen.** Simulations of sorption of binary mixtures comprised of $N_2$ and $O_2$ (80:20, respectively, in the gas phase) were carried out on the LiLSX-P-III+III′ structure at 298 K. The results are presented in Figure 11. For comparison, simulated results for the single component sorption are also included. Obviously, sorption of $N_2$ is increased while $O_2$ uptake is decreased in the mixture case, as compared to the single component sorption at any given pressure. Since the interaction between $N_2$ and the zeolite is much stronger than that between of $O_2$ and the zeolite, the presence of $N_2$ is expected to decrease the sorption capacity for $O_2$. However, it is not clear so far why $N_2$ uptake in a mixture occurs to exceed that for $N_2$ uptake in the single component sorption case. These results indicate that values of $N_2/O_2$ selectivity for a binary mixture case should also exceed those calculated from single component sorption isotherms.

In another set of simulations, the influence of the mole fraction of $N_2$ and $O_2$ on both sorption capacity and isosteric sorption heat was studied at 100 kPa. As shown in Figure 12, the $N_2$ sorption capacity increases with the gas-phase mole

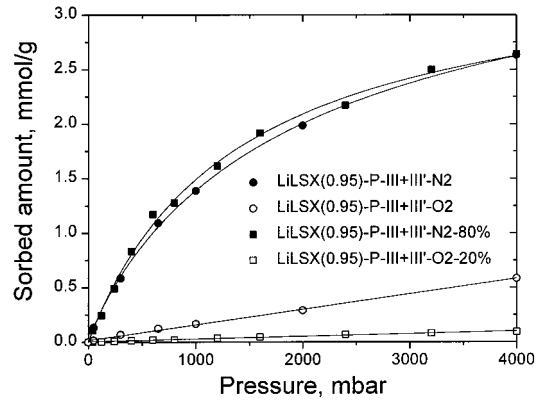


**Figure 11.** Simulated single component and mixture sorption isotherms for nitrogen and oxygen on LiLSX zeolite. The gas-phase mole fraction of oxygen is 0.20. The following charges were used: $q_{Li} = 0.95$, $q_{Al}$ and $q_{Si} = 1.525$, and $q_O = -1.0$.

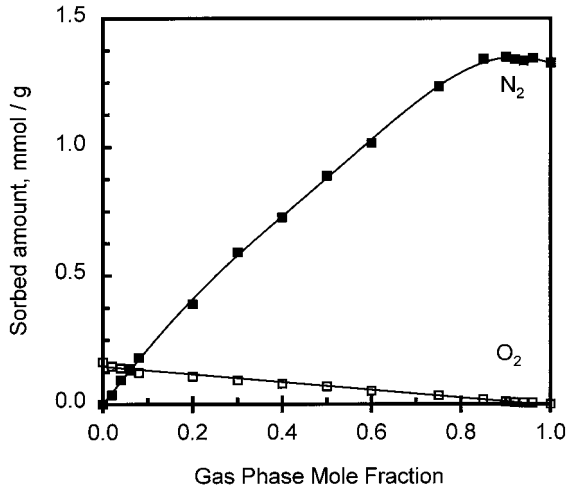


**Figure 12.** Simulated mixture sorption isotherms of nitrogen and oxygen on LiLSX as dependence on gas-phase mole fraction, at total gas pressure, $p = 100$ kPa. The following charges were used: $q_{Li} = 0.95$, $q_{Al}$ and $q_{Si} = 1.525$, and $q_O = -1.0$.

fraction, up to about 0.85. As the concentration of $N_2$ exceeds the value of mole fraction, 0.85, the $N_2$ capacity decreases slightly but gradually. This is consistent with the finding that the $N_2$ capacity for a (80:20) mixture of $N_2$ and $O_2$ is higher than that for single component $N_2$ sorption as reported in Figure 11. As expected, the sorption uptake for $O_2$ decreases with increase in gas-phase mole fraction for $N_2$. Similar experimental findings have been reported for other systems.[12]

Values of partial isosteric sorption heats of $N_2$ and $O_2$ obtained from simulation of mixture sorption equilibria as a function of *sorption phase* composition at total gas-phase pressure, $p = 100$ kPa, are plotted in Figure 13. The total isosteric sorption heat calculated using the equation, $\Delta H_m = \Sigma y_i \overline{\Delta H_i}$, was also included in Figure 13, where $y_i$ denotes the mole fraction of component i in the coexisting gaseous bulk phase.

The partial isosteric sorption heats of $N_2$ and $O_2$ are similar to those of the pure $N_2$ and $O_2$, respectively, and they are almost the same at any mole fraction. However, the total isosteric sorption heat is almost constant up to a sorbate composition of *c*. 60% $N_2$ and is nearly close to the value for pure $O_2$ sorption. At about a mole fraction of 0.85 for $N_2$, there is an exponential increase in the values of the isosteric heat of sorption. This phenomenon is mainly due to the higher gas-phase mole fraction of $O_2$ compared with that of $N_2$, due to the higher $N_2/O_2$

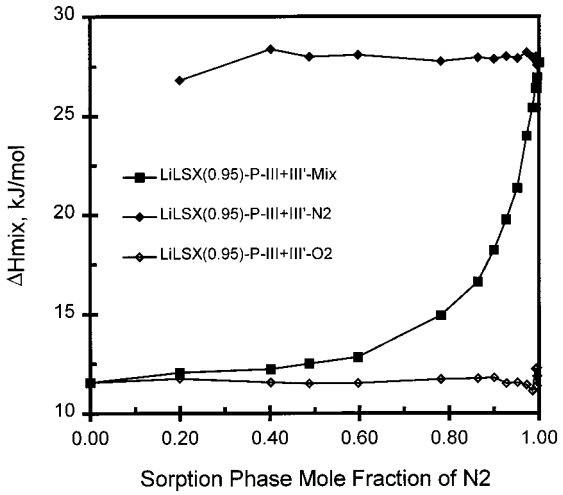


**Figure 13.** Simulated isosteric mixture sorption heats of nitrogen and oxygen on LiLSX as dependence on sorption phase mole fraction, at total gas pressure, $p = 100$ kPa. The following charges were used: $q_{Li} = 0.95$, $q_{Al}$ and $q_{Si} = 1.525$, and $q_O = -1.0$.

selectivity of LiLSX sorbent. Dependencies of sorption heats simulated for the mixture case are similar to corresponding experimental results published for another faujasite as described in ref 12.

## VI. Conclusions

Grand canonical Monte Carlo simulation of sorption of nitrogen and oxygen has been performed on LiLSX zeolite structures. The positions of Li cations in the LiLSX structure were predicted using the MSI Cerius$^2$ cation locator module. If proper partial charges are used on the framework atoms, the MSI cation locator allows for a reasonably good prediction of the positions of Li cations in the LSX structure. A very good match between the simulated and experimental sorption data was obtained on LiLSX using the Watanabe force field provided within the MSI Cerius$^2$ package, when the partial charge on Li cations was adjusted to 0.95. This refers, in particular, to values of isosteric sorption heats for nitrogen and oxygen.

Simulation of sorption on various simulated structures of LiLSX that contain Li cations at different locations indicates that sites SIII and SIII′ show similar values of interaction energy, which is particularly interesting with regard to nitrogen. The influence of the position of Li cations in sites either SIII or SIII′ on the calculated values of sorption capacity and isosteric sorption heat seems be less significant, indicating that the energy of both sites is almost the same. The analysis of the distribution of sorbing species clearly indicates that cations occupying site SII were not involved in the sorption process, to a remarkable extent.

In addition to isosteric sorption heats, the simulated values for sorption capacity and $N_2/O_2$ selectivity are in very good agreement with experimental data. The simulated values of sorption capacity and isosteric sorption heat on the predicted structures are close to those obtained on structures built by using literature crystal structure data and sorption data that were obtained experimentally at low pressures. Sorption isotherms simulated on LiLSX structures that were generated by means of the MSI cation locator were found to be close to those obtained on the structures built by using crystal structure and experimental sorption data. At lower pressures, they fit very well with the experimental data, but deviate by as much as 30 % at higher pressures partly due to fixed lattice calculations.

Simulated mixture sorption isotherms of nitrogen and oxygen showed an enhancement in nitrogen sorption while oxygen sorption was slightly suppressed as compared to the corresponding single component data. At a given pressure, the nitrogen sorption capacity increased with the mole fraction of nitrogen in the equilibrium gas phase, up to a value of 0.85, and then decreased gradually to the value of single component nitrogen sorption. On the other hand, oxygen sorption capacity decreases gradually with increasing mole fraction of nitrogen in the gas phase. The total isosteric sorption heat of nitrogen and oxygen sorption in a mixture is almost the same over a very broad range of gas-phase composition.

**Acknowledgment.** We thank Dr. A. F. Ojo for preparing the LiLSX powder sample, Z. Orban for measuring nitrogen and oxygen adsorption isotherms and The BOC Group for the permission to publish this work. Our special thanks are due Dr. D. MacLean, BOC Gases, for his support and encouragement, and to the referees for their valuable comments and suggestions.

## References and Notes

(1) June, R. L.; Bell, A. T.; Theodorou, D. N. *J. Phys. Chem.* **1990**, *94*, 8232; Woods, G. B.; Rowlinson, J. S. *J. Chem. Soc., Faraday Trans.* **1989**, *85*, 765.

(2) Bakaev, V. A.; Steele, W. A. *Langmuir* **1992**, *8*, 148.

(3) Cracknell, R.; Koh, C. A.; Thompson, S. M.; Gubbins, K. E. *Mater. Res. Soc. Proc.* **1993**, *290*, 135.

(4) Smit, B.; Siepmann, I. *Science* **1994**, *264*, 1118. Grant, G. H.; Abrahams, R. J. *Catalysis* **1989**, *8*, 68. Reichert, H.; Schmidt, W.; Grillet, Y.; Llewellyn, P.; Rouquerol, J.; Unger, K. K. *Stud. Surf. Sci. Catal.* **1994**, *87*, 517.

(5) Karavias, F.; Myers, A. L. *Mol. Simul.* **1991**, *8*, 23. Goodbody, S. J.; Watanabe, K.; MacGowan, D.; Walton, J. P. R. B.; Quirke, N. *J. Chem. Soc., Faraday Trans.* **1991**, *87*, 1951.

(6) Cracknell, R. F.; Gubbins, K. E. *Langmuir* **1993**, *9*, 824.

(7) Razmus, D. M.; Hall, C. K. *AIChE Journal* **1991**, *37*, 769.

(8) Watanabe, K.; Austin, N.; Stapleton, M. R. *Mol. Simul.* **1995**, *15*, 197.

(9) Richards, A. J.; Watanabe, K.; Austin, N.; Stapleton, M. R. *J. Porous Mater.* **1995**, *2*, 43. Newsam, J. M.; Freeman, C. M.; Gorman, A. M.; Vessal, B. *Chem. Commun.* **1996**, 1945.

(10) Ligniéres, J.; Pullumbi, P. In *Fundamentals of Adsorption*, Proceedings 6th International Conference on Fundamentals of Adsorption; Meunier, F., Ed.; Elsevier: Paris, 1998, p 719.

(11) Chao, C. C. U.S. Patent No. 4, 859,217, 1989. Coe, C. G.; Kirner, J. F.; Pierantozzi, R.; White, T. R. U.S. Patent. No. 5, 152,813, 1992. Fitch, F. R.; Bülow, M.; Ojo, A. F. U.S. Patent. No. 5, 464,467, 1995.

(12) Shen, D.; Bülow, M. *Microporous Mesoporous Mater.* **1998**, *22*, 237. Bülow, M.; Shen, D. In *Fundamentals of Adsorption*, Proceedings 6th International Conference on Fundamentals of Adsorption; Meunier, F.; Elsevier: Paris, 1998; p 87.

(13) Newsam, J. M.; Freeman, C. M.; Gorman, A. M.; Vessal, B. *Chem. Commun.* **1996**, 1945. Gorman, A. M.; Freeman, C. M.; Kölmel, C. M.; Newsam, J. M. *Faraday Discuss.* **1997**, *106*, 489. Ligniéres, J.; Newsam, J. M. *Microporous Mesoporous Mater.* **1999**, *28*, 305.

(14) Mellot, C. F.; Cheetham, A. K. In *Proceedings of the 12th International Zeolite Conference;* Treacy, M. M. J., Marcus, B. K., Bisher, M. E., Higgins, J. B., Eds.; Materials Research Society: Warrendale, PA, 1998; p 2766.

(15) Woods, G. B.; Rowlinson, J. S. *J. Chem. Soc., Faraday Trans.* **1989**, *85*, 765. Karavias, F.; Myers, A. L. **1991**, *8*, 23.

(16) Allen, M. P.; Tildesley, D. J. *Computer Simulation of Liquids*; Oxford University Press: New York, 1956.

(17) Plévert, J.; Di Renzo, F.; Fajula, F.; Chiari, G. *J. Phys. Chem.*, **1997**, *49*, 10340.

(18) Feuerstein, M.; Lobo, R. F. *Chem. Mater.* **1998**, *10*, 2197.

(19) Rege, S. U.; Yang, R. T. *Ind. Eng. Chem. Res.* **1997**, *36*, 5358.

(20) Coe, C. C. In *Access in Nanoporous Materials*; Pinnavaia, T. J., Thorpe, M. F., Eds.; Plenum Press: New York, 1995.

(21) Shen, D.; Jale, S. R.; Bülow, M.; Ojo, A. F. *Stud. Surf. Sci. Catal.* **1999**, *125*, 667.

(22) Jasra, R. V.; Choudary, N. V.; Bhat, S. F. T. *Ind. Eng. Chem. Res.* **1996**, *35*, 4221.

(23) Newsam, J. M.; Freeman, C. M.; Gorman, A. M.; Vessal, J. *Chem. Commun.* **1996**, 1945. Guliants, V. V.; Mullhaupt, J. T.; Newsam, J. M.; Gorman, A. M.; Freeman, C. M. *Catal. Today* **1999**, *50*, 661.

(24) Jaramillo, E.; Auerbach, S. M. *J. Phy. Chem. B* **1999**, *103*, 9589.

(25) Olson, D. H. *Zeolites* **1995**, *15*, 439.